Advanced Airborne Electromagnetics for Capturing Hydrogeological Parameters Over the Coastal Karst System of Tulum, Mexico

Arnulf Schiller, Robert Supper, Ingrid Schattauer, Klaus Motschka, Gonzalo Merediz Alonso and Alejandro Lopéz Tamayo

Abstract

The presented case study is part of a series of international research cooperations started in 2006 and still ongoing. The study area is located at the east coast of the Yucatan Peninsula, México, south of the city of Tulum including the northernmost part of the Sian Ka'an Biosphere Reserve. This study focuses on the third aero-electromagnetic (AEM) survey in the area conducted in January 2015 by the Geological Survey of Austria and Amigos de Sian Ka'an and on results prepared in course the Swiss–Mexican–Austrian project 'Xibalba'. AEM enables quick measurement of the distribution of electrical conductivity in the subsurface over difficult accessible terrain. By means of a common frequency-domain four-channel helicopter probe and application of newly developed data processing algorithms, signatures of karst conduits and aquifers could be resolved. It is shown that the methods are able to deliver crucial structural information about karst groundwater regimes with unique depth information compared to previous surveys.

P. Renard, C. Bertrand (Eds.), *EuroKarst 2016, Neuchâtel*, Advances in Karst Science,
DOI 10.1007/978-3-319-45465-8_4

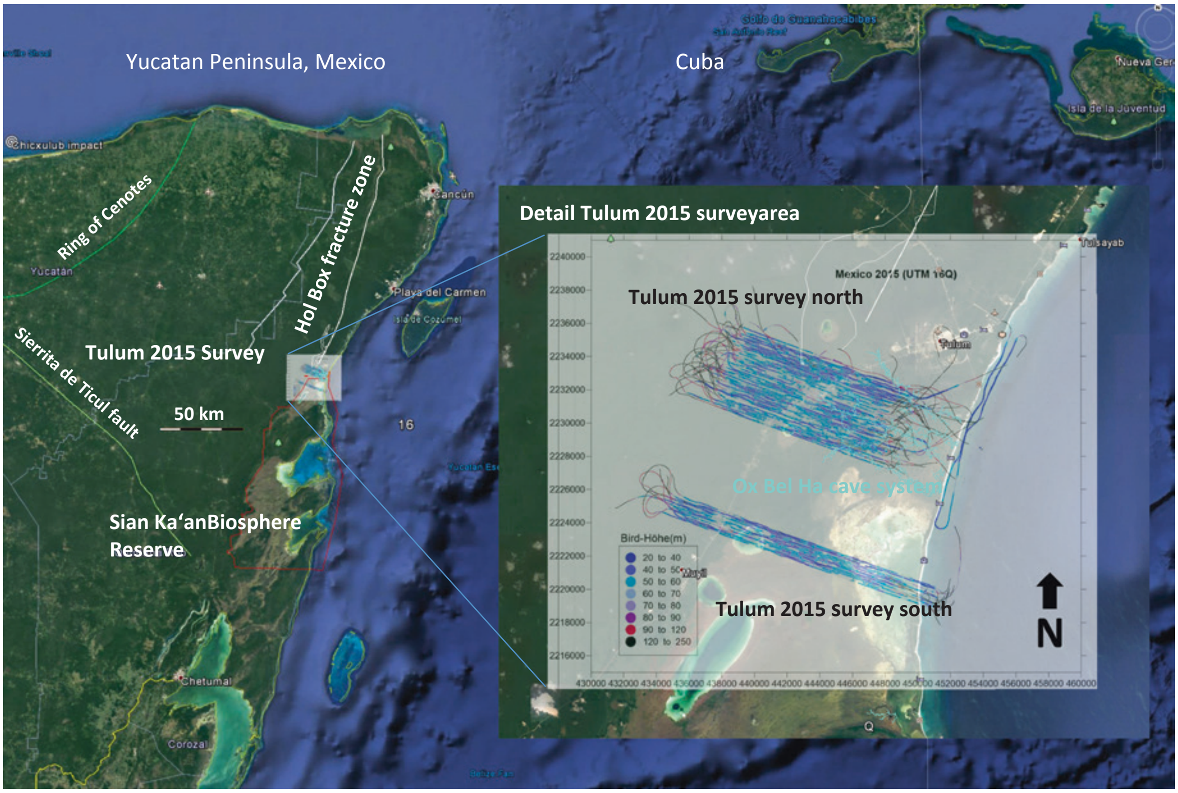

Fig. 4.1 North-east part of Yucatan Peninsula with survey area (*white*) and relevant fault zones. *Detail*: Flight lines with Ox Bel Ha cave system

4.1 Introduction

Karst aquifers represent an important water resource to a significant part of the earth's population. In the area of Tulum, the water resource is endangered by rapid urban development. Sustainable water management and protection of the nearby barrier reef and Sian Ka'an Biosphere Reserve require better understanding of the karst water system and its potential and dynamics. Important studies are given by Beddows (2004), Gondwe (2010) or Bauer-Gottwein et al. (2011). Our study is part of an ongoing series of international research cooperations started in 2006 adressing the general objectives of developing innovative data acquisition and numerical modelling methods for karst research (Vuilleumier et al. 2013).

Data acquisition is challenging due to difficult access to the conduit system, which is only possible through cenotes widely distributed in the jungle, few wells or boreholes (Supper et al. 2010). Hence, the idea was to assess and develop the applicability of airborne electromagnetics (AEM), which provides the advantage of quick, comfortable scanning of the underground beneath wide and difficult terrain with a helicopter-borne measurement system. The case study focused on herein concerns the latest AEM survey conducted in January 2015 by means of a common AEM probe combined with advanced AEM data processing.

4.2 Survey Area

The survey addresses the coastal karst plain south of Tulum town, which is mainly covered by jungle, wetland, lagoons and mangroves and exhibits very flat topography (Figs. 4.1 and 4.3). In the subsurface, the whole region is nerved by a vast network of underwater caves, partially surveyed by exploration divers (Figs. 4.1 and 4.6). The complex conduit network developed in nearly horizontally layered limestone predominantly during ice ages when the sea level was up to 100 m lower. The limestone reaches depths of several thousand metres and exhibits varying porosity, spanning from very compact to very porous, typical for young reef limestone. The caves or conduits seem to be concentrated mainly in the top 40 m. However, in some places there is indication of deeper systems (Meacham 2007). The topmost or freshwater layer of this groundwater regime actually represents the only freshwater resource of the region. Its thickness spans from zero at the coast to approximately 10–35 m, at distances to the coast reaching up to 25 km. Below the freshwater layer, there is salt water intruding from the sea and reaching deeper regions. The network is constrained inland to the northwest by the Holbox fracture zone (◘Figs. 4.1 and 4.6). Known outlets of the conduit network are located in the lagoons of the bio-reserve and between the beach and the barrier reef (Beddows 2004).

4.3 Objectives

In principle, karst aquifers are characterized by the presence of two distinct flow domains: limestone matrix and karst conduits. A flow model of karst aquifers requires detailed, spatially distributed information on the characteristics of these two domains. Methods, which determine the distribution of the electrical resistivity (or conductivity) in the subsurface, can provide such information. The potential of the AEM method for achieving this is already proven by two airborne surveys carried out in 2007 and 2008 (Schiller et al. 2013). The 2015 AEM survey was scheduled as an extension of these surveys to the south for treating following questions:

- Can the Holbox fracture zone be imaged by AEM?
- How do characteristics of the karst water regime change with distance to the coast?
- Are there conduit branches connecting the Ox Bel Ha system to the northern lagoons of the Sian Ka'an bio-reserve?
- How does the AEM method perform above lagoons, sea and reef?

4.4 Methods

4.4.1 Measurement System

AEM measures the electrical conductivity (=1/resistivity) distribution in the underground, which correlates with water saturation porosity and salinity (Reynolds 1997). The measurement system is an electromagnetic frequency-domain probe ('bird') towed 30 m below a helicopter. The bird is flown around 50 m above ground at a speed of 100–130 km/h. Transmitter coils in the front section of the bird transmit an electromagnetic field in four-frequency channels (400, 3200, 7200 and 28,800 Hz), which induces eddy currents in the subsurface. Receiver coils mounted in the rear section receive the sum of secondary field, radiating from the eddy currents in the ground and primary field of the transmitter. The secondary field is referred to the primary field in parts per million (ppm) of the primary field amplitude and by phase shift. During flight, measurement is taken ten times per second, which corresponds to a spacing of about 3 m in mean. The four-frequency field provides frequency-dependent depth penetration and thus depth information (Motschka 2001).

4.4.2 Flight Line Schedule

The 2015 survey is split into two parts (◘Figs. 4.1, 4.3 and 4.6). The northern part with approx. 10 × 5 km connects and overlaps partially the 2007 and 2008 surveys. The southern part is isolated with an extension of some 16 × 1.6 km covering jungle, dry steppe inland, a brackish lagoon and a near offshore part, partially including the reef. The flight line orientation is perpendicular to the coast (WNW to ESE, bearing 19.5°/289.5°, respectively). Line separation is 100 m. Flight altitude of the sensor above ground during measurement was kept between 40 and 50 m.

4.4.3 Data Processing

The applied data pre-processing comprises the following steps:

- Correcting for transmitter field variations and signal bias using higher altitude data.
- Signal drift reduction by evaluating height correlations of signal.
- Reducing residual signal drift artefacts by de-stripping algorithm.
- Inversion of pre-processed data for electrical conductivities of a 35-horizontal-layer model beneath each measurement by common 1d inversion (EM1DFM v1.0, developed at the University of British Columbia, Vancouver). Maximum model depth is 50 m.

Visualization of the inversion result is done by maps of horizontal depth slices and vertical sections as well as in 3d (◘Figs. 4.2, 4.3 and 4.5). Enhancing of structures and horizons is accomplished by filtering the inversion results for extracting significant horizons as well as enhancing indication for possible presence of conduits and caves, respectively (◘Fig. 4.6).

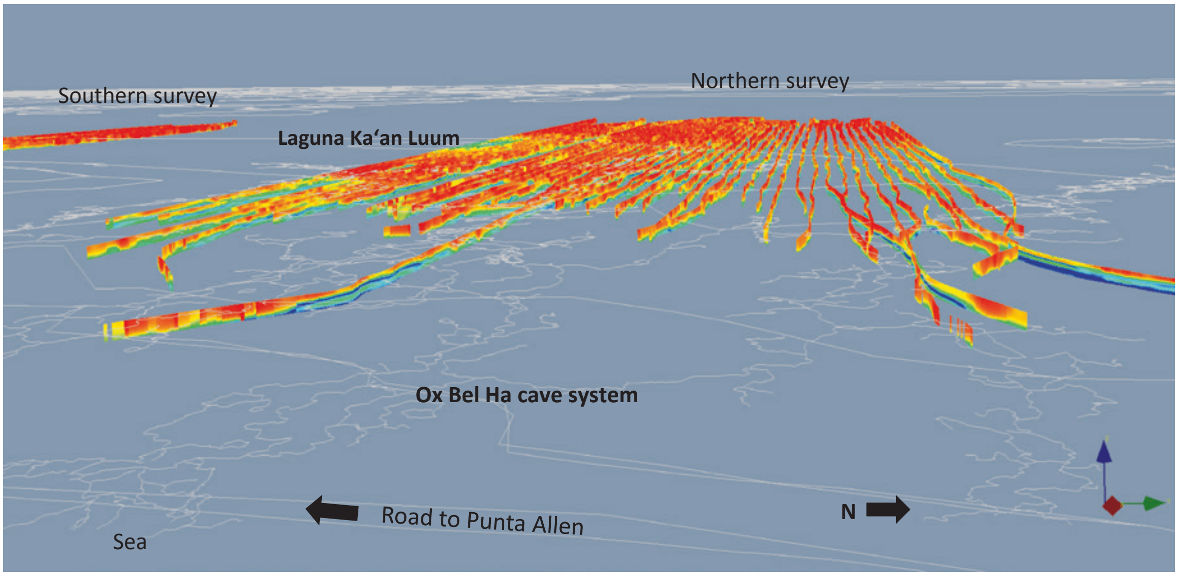

Fig. 4.2 Inversion results: AEM 2015 north (and part of south) in 3d visualization of measurement volume with *colour*-coded distribution of apparent electrical conductivity. *Blue* high conductivity, *red* low conductivity

4.5 Results and Interpretation

Pre-processed AEM data have been inverted for vertical distribution of electrical conductivity in the underground beneath each measurement point. The inversion model was defined with twenty layers of 1-m thickness down to 20 m depth, followed by 15 layers of 2-m thickness down to 50 m depth.

4.5.1 Layer Structure

In most sections of the southern survey as well as in part of the sections of the northern survey, a distinct high conductivity layer is visible. In the near offshore area, it is related to top water layer. In lagoons, it indicates the brackish top layer. In some sections of the southern survey, the layer declines inland rapidly (line TUL111 in Fig. 4.5). This could represent part of a fault related to the Holbox fracture zone. The location of the declining horizon is also marked in Figs. 4.4 and 4.6. The drop of the high conductive layer can be followed down to depths of 45 m. This high contrast layer most probably coincides with top of the saline aquifer, hence partially with the halocline. If interpreted this kind, one learns that the halocline significantly changes from zero in the sea-connected lagoons to minus 15 m below dry inland and down to depths of 35 m and more at certain locations inland. This indicates heterogenic limestone forming relatively isolated halocline basins and freshwater pushing seawater down. Finding from this analysis is a picture much more complex than assumed in previous interpretation.

4.5.2 Conduits

Similar to reprocessing of the 2007 and 2008 AEM survey data, a filter was applied for enhancing possible conduits (Schiller et al. 2013). Result is a map indicating the presence of conduits. Generally, conduit detection strongly depends on the direction of lines with respect to the predominant orientation of the conduit system (direction sensitivity). The sensitivity is best if the angle is near 90°. This is evident since the separation between measurement points along a line is about 3 m, while it is 100–200 m between the lines. In the case of the 2015 survey, the direction was chosen perpendicular to the coastline in order to detect potential Holbox fractures. This produced gracing cuts between flight lines and main conduit branches. Hence, the sensitivity for sea-orientated cave systems was reduced by the flight line orientation. Components of the conduit systems orientated more parallel to the coastline could be detected with higher sensitivity

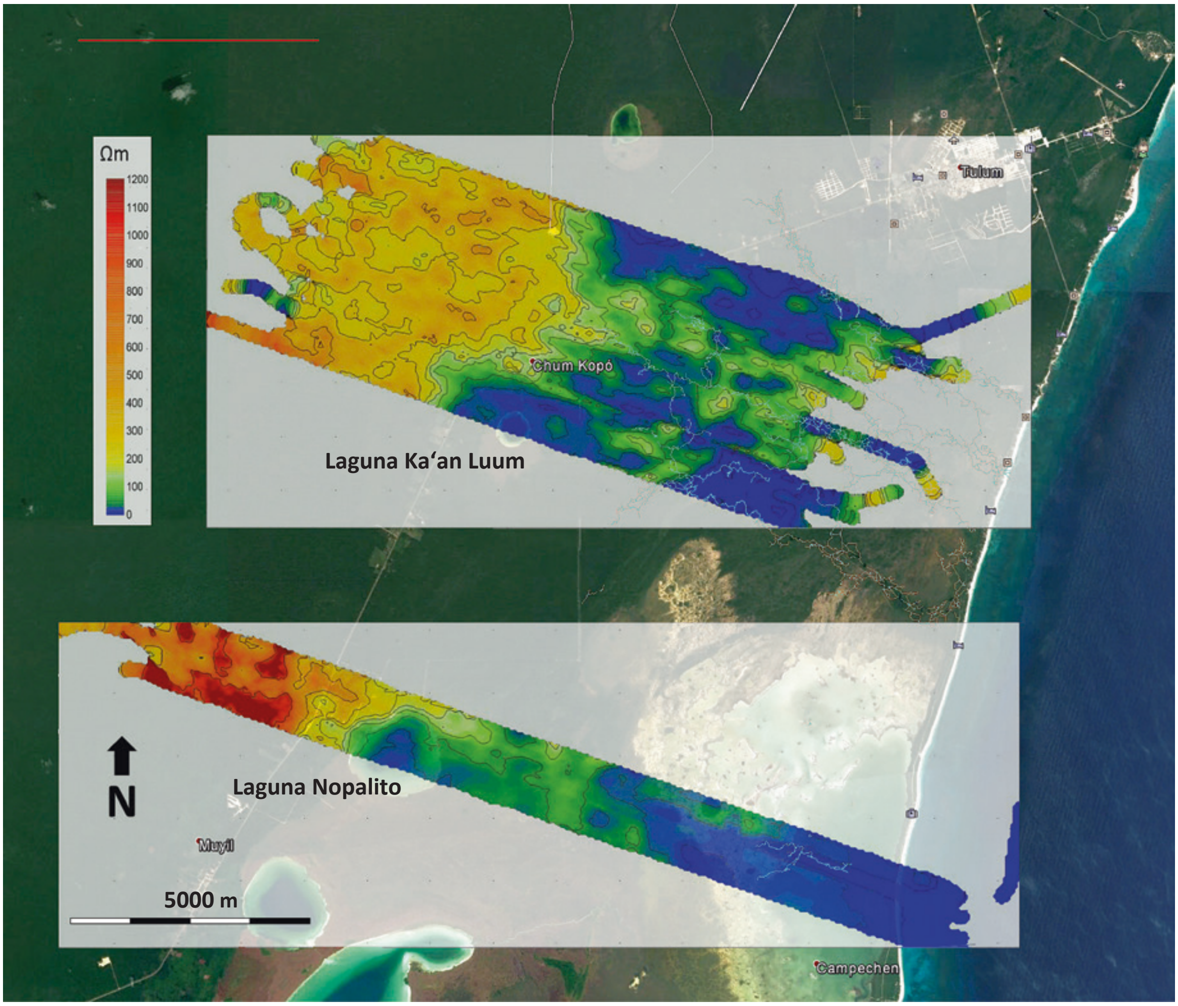

Fig. 4.3 Inversion results: Apparent resistivity of 25 m depth layer. Overlay with satellite imagery (Google Earth). *Blue lines* cave survey of Ox Bel Ha system

as in the 2007 and 2008 surveys, providing completing information (Fig. 4.6). The overall picture of the ppm-maps seems to be noisy. Still, inversion results correlate significantly with surveyed caves. Evaluation in the 25-m layer of northern inversion as shown in Fig. 4.3 gives 75–85 % positive correlation. Furthermore, underwater cave surveys are restricted to accessible parts of the system. The underwater survey is done by dead-reckoning technique, and over a long distance, positioning errors can sum to the size of lateral noise granules in the AEM maps degrading correlation as well. Basic question is how much of the noisy features are caused by system noise and how much images the stochastic characteristics of the karst features. These questions are worth being investigated in course of further studies. One remarkable feature is shown in Fig. 4.6. The map indicates a conduit propagating from the new urban waste deposit right to the south, possibly discharging into the middle and south branch of the Ox Bel Ha system. If that proves true, possible contamination caused by insulation leaks could spread fast and affect a large area also including the barrier reef in short time. Sections above known caves show low-conductivity features correlated with the surveyed caves even above brackish lagoons (Fig. 4.7). This is remarkable since brackish or seawater was always suspected to shield the EM field and consequently decreases the depth penetration of the method. In our results, structures are resolvable in the saltwater body down to 50 m depth.

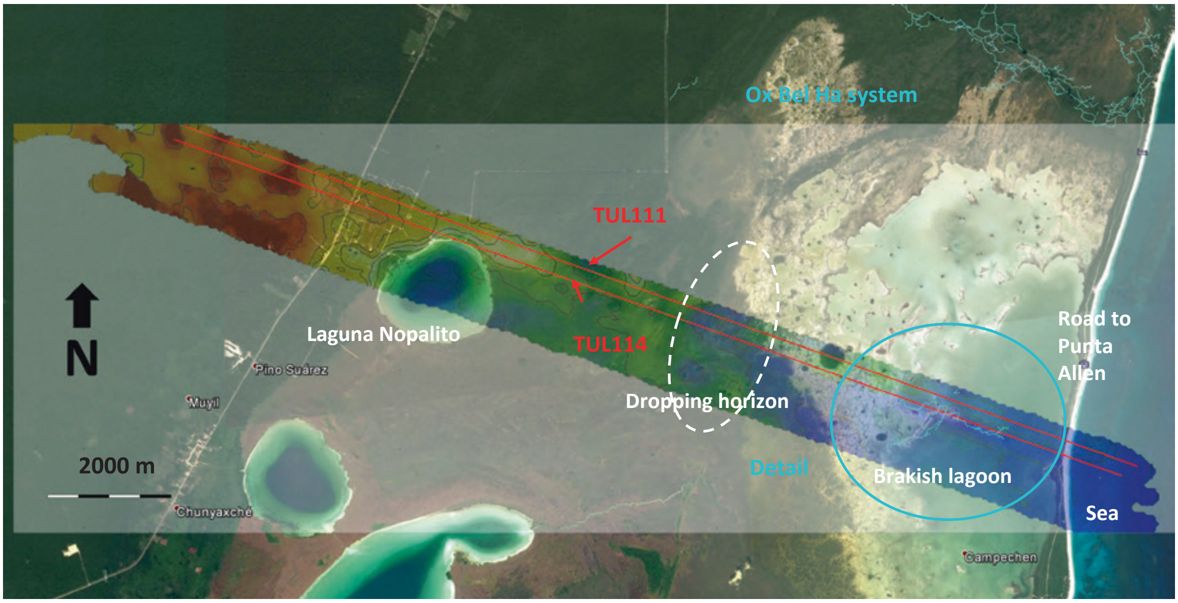

Fig. 4.4 South survey: Inversion for 25 m depth with lines TUL 111 and 114. Overlay with satellite imagery (Google Earth)

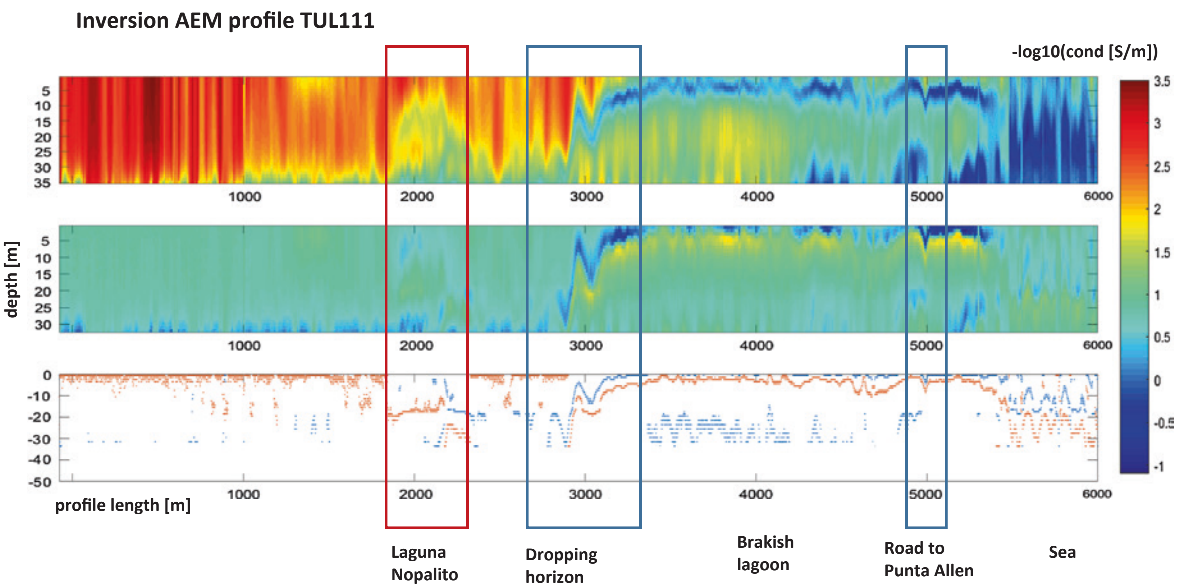

Fig. 4.5 South survey: inversion result—depth section of line TUL111—*top* conductivity, *middle* vertical gradient, *bottom* horizons extracted from vertical gradient

4

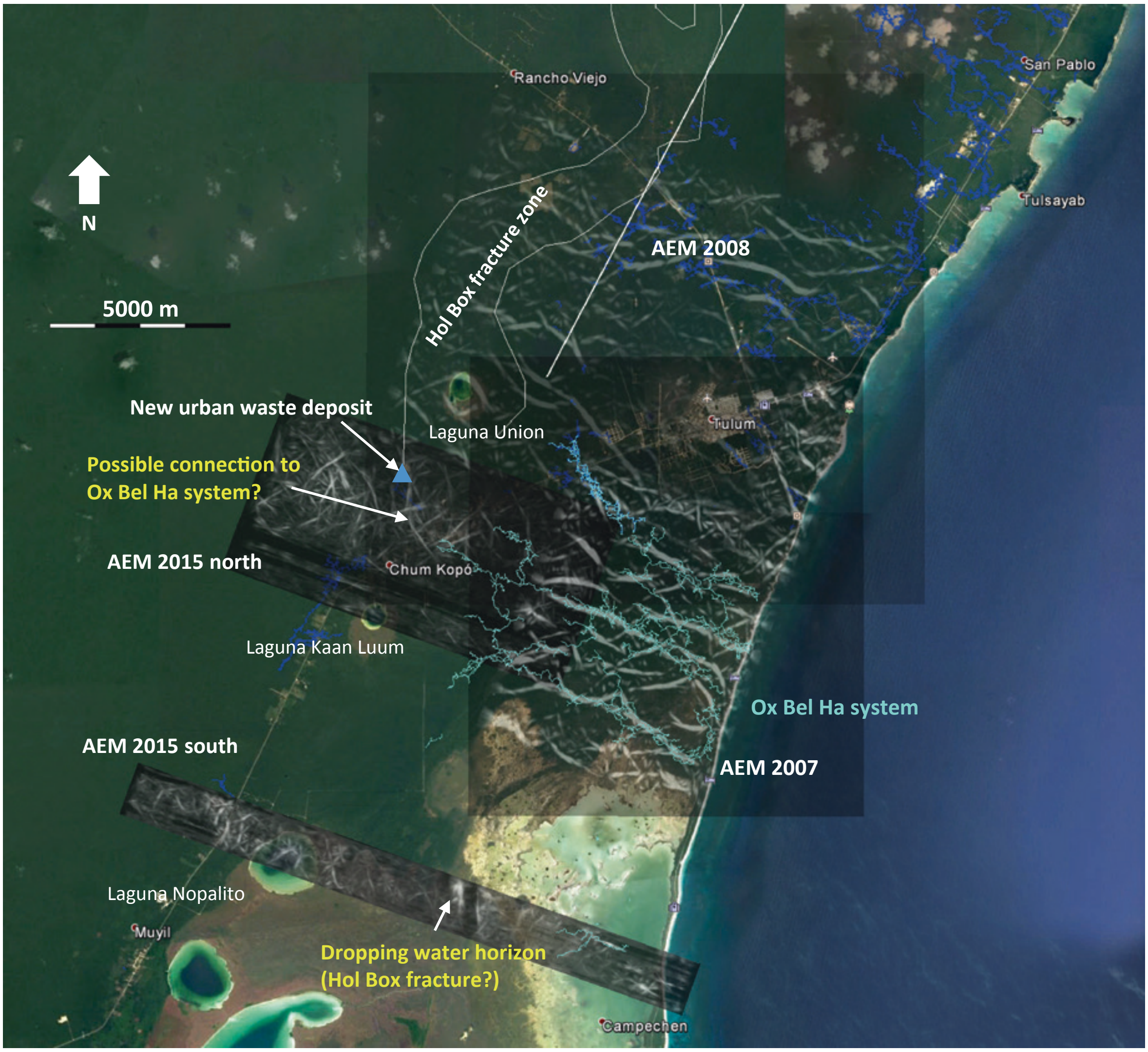

Fig. 4.6 Combined conduit maps of 2007, 2008 and 2015 surveys

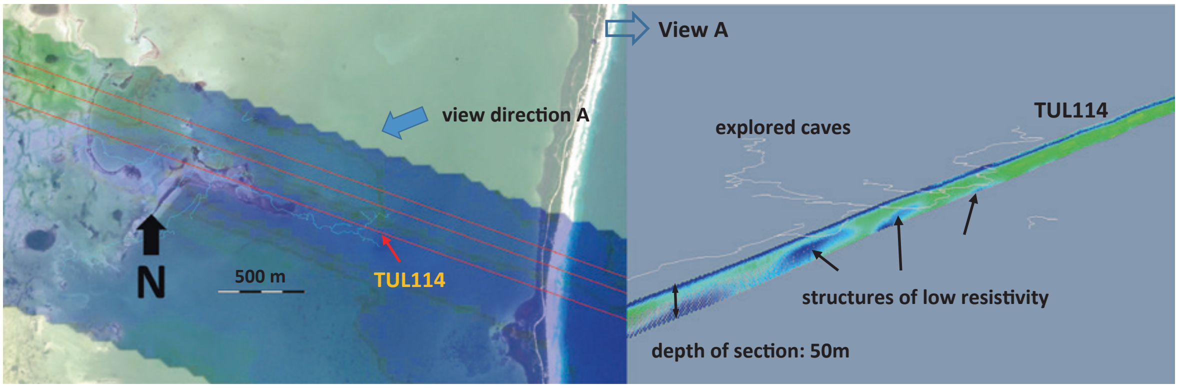

Fig. 4.7 Detail of line TUL114. *Right* perspective view to section cutting known caves

4.6 Conclusion

Advanced processing methods enabled extraction of much more information about the karst water regime from AEM data than experienced in previous studies. Complex layering is imaged indicating a complex shape of the halocline table and deeper seawater distribution. The conduit map of the 2015 survey shows less organization of the conduit component parallel to the coast confirming the main conduit systems being directed to the sea according with the 2007 and 2008 survey results and exploration dive surveys. In the southern survey area, a significant drop of saline water layers approximately 7 km inland images a structure possibly related to the Holbox fracture zone. Furthermore, there is evidence of a conduit branch connecting from the location of the new waste deposit to the Ox Bel Ha system. Proper AEM processing gave readable information about layering and structures beneath lagoons, the reef and the sea. Therefore, the AEM method combined with advanced data processing proves to be a valuable tool for investigations in karst as well as in coastal areas.

Acknowledgments Thank is expressed to Robert and Richard Schmittner (Xibalba Diving Center), as well as Bil Phillips (Speleotech) for providing cave survey data and great support. The research was financed by the Austrian Science Fund (FWF project I994-N29).

References

Beddows, P.A. (2004) Groundwater hydrology of a coastal conduit carbonate aquifer: Caribbean coast of the Yucatán Peninsula, México. PhD Thesis, University of Bristol, Bristol, 303 pp

Gondwe, B.R.N. (2010) Exploration, modelling and management of groundwater-dependent ecosystems in karst – the Sian Ka'an case study, Yucatan, Mexico. PhD Thesis, Technical University of Denmark, Kongens Lyngby, 86 pp

Bauer-Gottwein, P. et al. (2011) Review: The Yucatán Peninsula karst aquifer, Mexico, Hydrogeology Journal, 19(3), 507–524

Vuilleumier, C., A. Borghi, P. Renard, D. Ottowitz, A. Schiller, R. Supper, and F. Cornaton, 2013, A method for the stochastic modeling of karstic systems accounting for geophysical data: an example of application in the region of Tulum, Yucatan Peninsula (Mexico). Hydrogeology Journal. 21(3):529–544

Supper, R., Schiller, A., Jochum, B., Ottowitz D. (2010) Geophysikalische Messungen in Tulum (Mexiko) – 2010, Österreichische Akademie der Wissenschaften, online-ISBN: 978-37001-6971-0, doi:10.1553/mab-geophys-tulum-2010

Meacham, S (2007) Freshwater Resources in the Yucatan Peninsula, in 'Sustainable Management of Groundwater in Mexico', Proceedings of a workshop (Series: Strengthening Science Based Decision Making in Developing Countries, The National Academic Press, pp 6–12 ISBN: 978-0-309-10582, DOI:10.17226/11875

Schiller, A., Supper, R., Merediz Alonso, G., Ottowitz, D., Vuilleumiere, C., Motschka, K. (2013) Aeroelectromagnetic mapping of the hidden ground water conduit systems beneath the Tulum Karst plains. IAGA, 12th Scientific Assembly, Merida, August 26–31, 2013, abstracts 1.3-7, abstract volume p. 102.

Reynolds, J. M. 1997, An Introduction to Applied and Environmental Geophysics, John Wiley & Sons Inc., ISBN 0–471-95555-8.

Motschka, K. (2001) Aerogeophysics in Austria. Bull Geol Surv Jpn 52(2/3):83–88